

# FUNDAMENTAL LIMITATIONS OF THE SASE FEL PHOTON BEAM POINTING STABILITY

E.A. Schneidmiller, M.V. Yurkov, DESY, Hamburg, Germany

## Abstract

The radiation from Self Amplified Spontaneous Emission Free Electron Laser (SASE FEL) [1, 2] has always limited value of the degree of transverse coherence. Two effects define the spatial coherence of the radiation: the mode competition effect, and the effect of poor longitudinal coherence. For the diffraction limited case we deal mainly with the effect of the poor longitudinal coherence leading to significant degradation of the spatial coherence in the post-saturation regime. When transverse size of the electron beam significantly exceeds diffraction limit, the mode competition effect does not provide the selection of the ground mode, and spatial coherence degrades due to contribution of the higher azimuthal modes. Another consequence of this effect are fluctuations of the spot size and pointing stability of the photon beam. These fluctuations are fundamental and originate from the shot noise in the electron beam. The effect of pointing instability becomes more pronouncing for shorter wavelengths. Our study is devoted to the analysis of this effect and description of possible means for improving the degree of transverse coherence and the pointing stability.

## INTRODUCTION

Previous studies have shown that coherence properties of the radiation from SASE FEL strongly evolve during the amplification process [3–7]. At the initial stage of amplification the spatial coherence is poor, and the radiation consists of a large number of transverse modes [7–15]. Longitudinal coherence is poor as well [16–18]. In the exponential stage of amplification the transverse modes with higher gain dominate over modes with lower gain when the undulator length progresses. This feature is also known as the mode competition process. Longitudinal coherence also improves in the high gain linear regime [18–20]. The mode selection process stops at the onset of the nonlinear regime, and the maximum values of the degree of the transverse coherence and of the coherence time are reached at this point. The undulator length required to reach saturation is in the range from about nine (hard x-ray SASE FELs) to eleven (visible range SASE FELs) field gain lengths [3]. The situation with the transverse coherence is favorable when the relative separation of the field gain between fundamental and higher modes exceeds 25-30%. In this case the maximum degree of transverse coherence can exceed the value of 90% [3, 7]. Further development of the amplification process in the nonlinear stage leads to visible degradation of the coherence properties.

Relative separation of the gain of the FEL radiation modes depends on the value of the diffraction parameter. Increase of the value of the diffraction parameter results in a smaller

relative separation of the gain of the modes. In this case we deal with the mode degeneration effect [9, 12]. Since the number of gain lengths to saturation is limited, the contribution of the higher spatial modes to the total power grows with the value of the diffraction parameter, and the transverse coherence degrades. Large values of the diffraction parameter are typical for SASE FELs operating in the hard x-ray wavelength range [21–25].

In this paper we perform analysis of the radiation modes, and find their ranking in terms of the field gain. The main competitor of the ground TEM<sub>00</sub> is the first azimuthal TEM<sub>10</sub> mode. When contribution of TEM<sub>10</sub> mode to the total power exceeds a few per cent level, a fundamental effect of bad pointing stability becomes to be pronouncing. The power of the effect grows with the electron beam size in the undulator. We present detailed analysis of this effect for Free Electron Laser FLASH [26, 27] which currently takes place due to the weak focusing in the undulator resulting in large values of the diffraction parameter and conditions of the "cold" electron beam [28]. Our analysis shows that operation with a stronger focusing of the electron beam and a lower peak current would allow one to improve both, the degree of transverse coherence and the pointing stability of the photon beam at FLASH.

The figure of merit for operation of optimized SASE FEL is the ratio of the geometrical emittance to the radiation wavelength,  $\hat{\epsilon} = 2\pi\epsilon/\lambda$  [3–5]. Parameter space of optimized SASE FELs is typical for the hard x-ray regime. We show that SASE FELs operating at short wavelengths and low electron beam energy with the value of  $\hat{\epsilon} > 1$  suffer from the mode degeneration effect resulting in significant degradation of the spatial coherence and pointing stability of the photon beam. The effect of the photon beam pointing jitter is a fundamental one, and can not be eliminated by eliminating of the jitters of machine parameters.

## ANALYSIS OF THE RADIATION MODES

We consider an axisymmetric model of the electron beam. It is assumed that the transverse distribution function of the electron beam is Gaussian, so the rms transverse size of matched beam is  $\sigma = \sqrt{\epsilon\beta}$ , where  $\epsilon$  is the rms beam emittance and  $\beta$  is the beta-function. In the framework of the three-dimensional theory, the operation of a short-wavelength FEL amplifier is described by the following parameters: the diffraction parameter  $B$ , the energy spread parameter  $\hat{\Lambda}_T^2$ , the betatron motion parameter  $\hat{k}_\beta$  and detuning parameter  $\hat{C}$  [11, 12]:

$$\begin{aligned} B &= 2\Gamma\sigma^2\omega/c, & \hat{C} &= C/\Gamma, \\ \hat{k}_\beta &= 1/(\beta\Gamma), & \hat{\Lambda}_T^2 &= (\sigma_E/E)^2/\rho^2, \end{aligned} \quad (1)$$

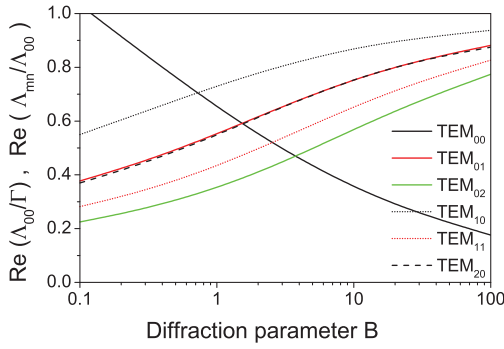


Figure 1: Ratio of the maximum gain of the higher modes to the maximum gain of the fundamental mode  $\text{Re}(\Lambda_{mn})/\text{Re}(\Lambda_{00})$  versus diffraction parameter  $B$ . The energy spread parameter is  $\hat{\Lambda}_T^2 \rightarrow 0$ , and the betatron motion parameter is  $\hat{k}_\beta \rightarrow 0$ . Color codes refer to the radial index of the mode: 0 - black, 1 - red, 2 - green. Line type codes refer to the azimuthal index of the mode: 0 - solid line, 1 - dotted line, 2 - dashed line. Black solid line shows the gain of the fundamental mode  $\text{Re}(\Lambda_{00})/\Gamma$ .

where  $E = \gamma mc^2$  is the energy of electron,  $\gamma$  is relativistic factor,  $\Gamma = [I\omega^2\theta_s^2 A_{JJ}^2 / (I_A c^2 \gamma_z^2 \gamma)]^{1/2}$  is the gain parameter,  $\rho = c\gamma_z^2 \Gamma / \omega$  is the efficiency parameter, and  $C = 2\pi / \lambda_w - \omega / (2c\gamma_z^2)$  is the detuning of the electron with the nominal energy  $E_0$ . Note that the efficiency parameter  $\rho$  entering equations of three dimensional theory relates to the one-dimensional parameter  $\rho_{1D}$  as  $\rho_{1D} = \rho / B^{1/3}$  [12, 29]. The following notations are used here:  $I$  is the beam current,  $\omega = 2\pi c / \lambda$  is the frequency of the electromagnetic wave,  $\lambda_w$  is undulator period,  $\theta_s = K / \gamma$ ,  $K$  is the rms undulator parameter,  $\gamma_z^{-2} = \gamma^{-2} + \theta_s^2$ ,  $I_A = mc^3 / e = 17$  kA is the Alfven current,  $A_{JJ} = 1$  for helical undulator and  $A_{JJ} = J_0(K^2/2(1+K^2)) - J_1(K^2/2(1+K^2))$  for a planar undulator.  $J_0$  and  $J_1$  are the Bessel functions of the first kind. The energy spread is assumed to be Gaussian with the rms deviation  $\sigma_E$ .

The amplification process in SASE FEL starts from the shot noise in the electron beam. At the initial stage of amplification, the coherence properties are poor, and the radiation consists of a large number of transverse and longitudinal modes [7–15]:

$$\begin{aligned} \vec{E} &= \sum_{m,n} \int d\omega A_{mn}(\omega, z) \Phi_{mn}(r, \omega) \\ &\times \exp[\Lambda_{mn}(\omega)z + im\phi + i\omega(z/c - t)]. \quad (2) \end{aligned}$$

Each mode is characterized by the eigenvalue  $\Lambda_{mn}(\omega)$  and the field distribution eigenfunction  $\Phi_{mn}(r, \omega)$ . The real part of the eigenvalue  $\text{Re}(\Lambda_{mn}(\omega))$  is referred to as the field gain. The field gain length is  $L_g = 1/\text{Re}(\Lambda_{mn}(\omega))$ . Eigenvalues and eigenfunctions are the solutions of the eigenvalue equation [10, 11]. Each eigenvalue has a maximum at a certain frequency (or, at a certain detuning), so that the detuning for each mode is chosen automatically in the case of a SASE

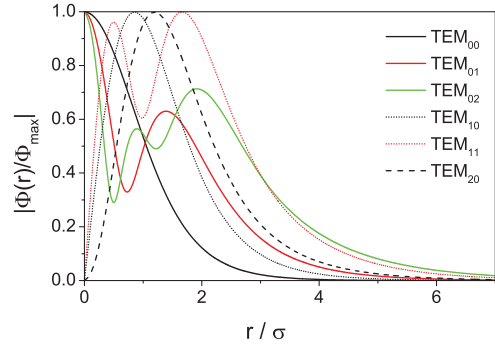
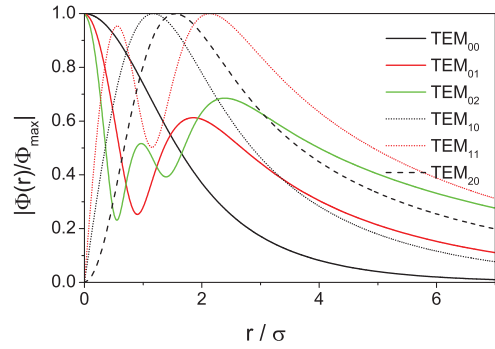


Figure 2: Amplitude of the eigenfunctions of the FEL radiation modes,  $|\Phi_{mn}(r)|/|\Phi_{\max}|$ . Top and bottom plots correspond to the diffraction parameter  $B = 1$  and  $B = 10$ , respectively. The detuning corresponds to the maximum of the gain. The energy spread parameter is  $\hat{\Lambda}_T^2 \rightarrow 0$ , and the betatron motion parameter is  $\hat{k}_\beta \rightarrow 0$ . Color codes refer to the radial index of the mode: 0 - black, 1 - red, 2 - green. Line type codes refer to the azimuthal index of the mode: 0 - solid line, 1 - dotted line, 2 - dashed line.

FEL (in contrast with seeded FELs where the detuning can be set to any value). Thus, we use the three dimensionless parameters:  $B$ ,  $\hat{k}_\beta$ , and  $\hat{\Lambda}_T^2$ .

Let us look closer at the properties of the radiation modes. The gains for several modes are depicted in Fig. 1 as functions of the diffraction parameter. The values for the gain correspond to the maximum of the scan over the detuning parameter  $\hat{C}$ . The curve for the  $\text{TEM}_{00}$  mode shows the values of the normalized gain  $\text{Re}(\Lambda_{00})/\Gamma$ . Curves for the higher spatial modes present the ratio of the gain of the mode to the gain of the fundamental mode,  $\text{Re}(\Lambda_{mn})/\text{Re}(\Lambda_{00})$ . Sorting the modes by the gain results in the following ranking:  $\text{TEM}_{00}$ ,  $\text{TEM}_{10}$ ,  $\text{TEM}_{01}$ ,  $\text{TEM}_{20}$ ,  $\text{TEM}_{11}$ ,  $\text{TEM}_{02}$ . The gain of the fundamental  $\text{TEM}_{00}$  mode is always greater than the gain of higher order spatial modes. The difference in the gain between the fundamental  $\text{TEM}_{00}$  mode and higher spatial modes is pronounced for small values of the diffraction parameter  $B \lesssim 1$ . The gain of higher spatial modes approaches asymptotically the gain of the fundamental mode for large values of the diffraction parameter. In other words, the effect of the mode degeneration takes place. Its origin can be understood with the qualitative analysis of the eigenfunctions (distribution of the radiation field in the near zone). Figure 2

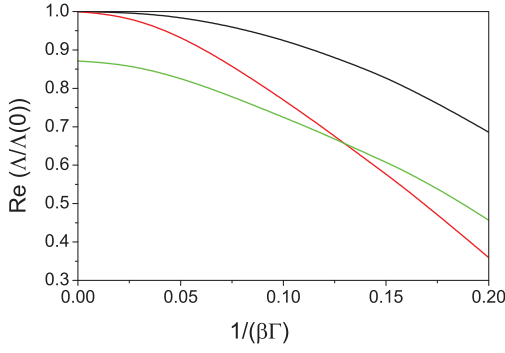


Figure 3: Dependence of the gain of TEM<sub>00</sub> mode (black curve) and TEM<sub>10</sub> mode (red curve) on the betatron motion parameter  $\hat{k}_\beta = 1/(\beta\Gamma)$ . The values are normalized to those at  $\hat{k}_\beta \rightarrow 0$ . Green curve shows the ratio of the gain of TEM<sub>10</sub> mode to the gain of TEM<sub>00</sub> mode. The diffraction parameter is  $B = 10$ . The energy spread parameter is  $\hat{\Lambda}_T^2 \rightarrow 0$ .

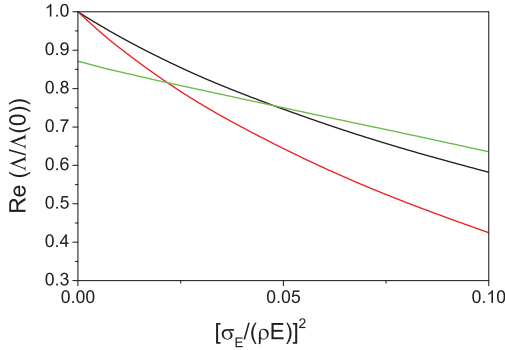


Figure 4: Dependence of the gain of TEM<sub>00</sub> mode (black curve) and TEM<sub>10</sub> mode (red curve) on the energy spread parameter  $\hat{\Lambda}_T^2$ . The values are normalized to those at  $\hat{\Lambda}_T^2 \rightarrow 0$ . Green curve shows the ratio of the gain of TEM<sub>10</sub> mode to the gain of TEM<sub>00</sub> mode. The diffraction parameter is  $B = 10$ . The betatron oscillation parameter is  $\hat{k}_\beta \rightarrow 0$ .

shows eigenfunctions of the FEL radiation modes for two values of the diffraction parameter,  $B = 1$  and  $B = 10$ . We observe that for small values of the diffraction parameter the field of the higher spatial modes spans far away from the core of the electron beam while the fundamental TEM<sub>00</sub> mode is more confined. This feature provides a higher coupling factor of the radiation with the electron beam and higher gain. For large values of the diffraction parameter all radiation modes shrink to the beam axis which results in an equalizing of coupling factors and of the gain. Asymptotically, the eigenvalues of all modes tends to the one dimensional asymptote as [5]:

$$\Lambda_{mn}/\Gamma \simeq \frac{\sqrt{3} + i}{2B^{1/3}} - \frac{(1 + i\sqrt{3})(1 + n + 2m)}{3\sqrt{2}B^{2/3}} \quad (3)$$

For a SASE FEL, the undulator length to saturation is in the range from about nine (hard x-ray range) to eleven (visible range) field gain lengths [3,4,6]. The mode selection

process stops at the onset of the nonlinear regime, about two field gain lengths before saturation. Let us make a simple estimate for the value of the diffraction parameter  $B = 10$  and a cold electron beam,  $\hat{\Lambda}_T^2 \rightarrow 0$ , and  $\hat{k}_\beta \rightarrow 0$ . We get from Fig. 1 that the ratio of the gain  $\text{Re}(\Lambda_{10}/\Lambda_{00})$  is equal to 0.87. With an assumption of similar values of coupling factors, we find that the ratio of the field amplitudes at the onset of the nonlinear regime is about of factor of 3 only. An estimate for the contribution of the higher spatial modes to the total power is about 10 %. Another numerical example for  $B = 1$  gives the ratio  $\text{Re}(\Lambda_{10}/\Lambda_{00}) = 0.73$ , and the ratio of field amplitudes exceeds a factor of 10. Thus, an excellent transverse coherence of the radiation is not expected for SASE FEL with diffraction parameter  $B \gtrsim 10$  and a small velocity spread in the electron beam.

Longitudinal velocity spread due to the energy spread and emittance serves as a tool for the selective suppression of the gain of the higher spatial modes [9,12]. Figures 3 and 4 show the dependence of the gain of TEM<sub>00</sub> and TEM<sub>10</sub> modes on the betatron motion parameter and the energy spread parameter. We see that with the fixed value of the diffraction parameter, the mode degeneration effect can be relaxed at the price of gain reduction. The situation with transverse coherence is favorable when relative separation of the gain between the fundamental and higher spatial modes is more than 25-30 %. In this case the degree of transverse coherence can reach values above 90% in the end of the high gain linear regime [5,7]. Further development of the amplification process in the nonlinear stage leads to a significant degradation of the spatial and of the temporal coherence [3,4,6].

## FLASH

In the present experimental situation, many parameters of the electron beam at FLASH depend on practical tuning of the machine [27]. Analysis of measurements and numerical simulations shows that depending on the tuning of the machine, the emittance may change from about 1 to about 1.5 mm-mrad. Tuning at small charges may allow one to reach smaller values of the emittance down to 0.5 mm-mrad. Peak current may change in the range from 1 kA to 2 kA depending on the tuning of the beam formation system. An estimate for the local energy spread is  $\sigma_E [\text{MeV}] \simeq 0.1 \times I [\text{kA}]$ . The average beta function in the undulator is about 10 meters.

Let us choose the reference working point with the radiation wavelength 8 nm, rms normalized emittance 1 mm-mrad and beam current 1.5 kA. Parameters of the problem for this reference point are: the diffraction parameter is  $B = 17.2$ , the energy spread parameter  $\hat{\Lambda}_T^2 = 1.7 \times 10^{-3}$ , betatron motion parameter  $\hat{k}_\beta = 5.3 \times 10^{-2}$ . Then the reduced parameters at other working points can be easily recalculated using the scaling:

$$B \propto \frac{\epsilon_n \beta I^{1/2}}{\lambda^{1/4}}, \quad \hat{k}_\beta \propto \frac{1}{\beta I^{1/2} \lambda^{1/4}}, \quad \hat{\Lambda}_T^2 \propto I \lambda^{1/2}.$$

Analyzing these simple dependencies in terms of their effect on mode separation, we can state that

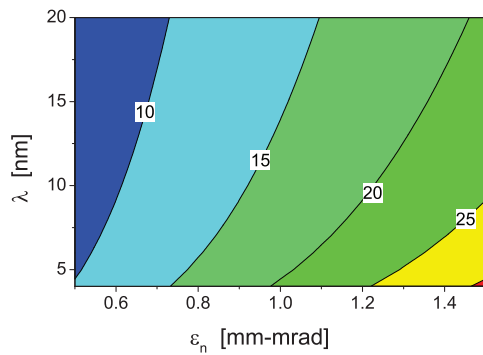


Figure 5: FLASH: contour plot for the value of the diffraction parameter  $B$  versus normalized emittance and radiation wavelength. Beam current is 1.5 kA, beta function is 10 m.

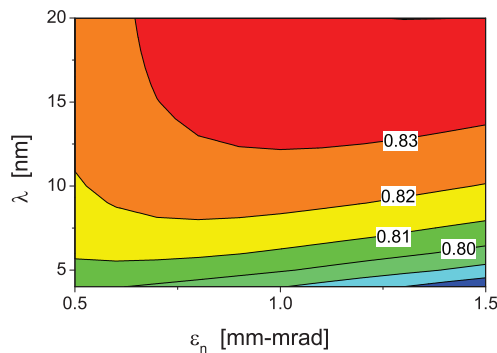


Figure 6: FLASH: contour plot of the ratio of the maximum field gain of  $TEM_{10}$  to the field gain of the ground  $TEM_{00}$  mode versus radiation wavelength and emittance. Beam current is 1.5 kA, beta function is 10 m.

- Dependencies on the wavelength are relatively weak (except for  $(\hat{\Lambda}_T^2)_{eff}$ ), i.e. one should not expect a significantly better transverse coherence at longer wavelengths. Moreover, mode separation can even be somewhat improved at shorter wavelengths due to a significant increase in  $(\hat{\Lambda}_T^2)_{eff}$ .
- Reduction of the peak current (by going to a weaker bunch compression) would lead to an improvement of mode separation (even though the energy spread parameter would be smaller). Obviously, the peak power at the saturation would be reduced.
- Dependence on the normalized emittance is expected to be weak because of the two competing effects. Mode separation due to a change of the diffraction parameter can be to a large extent compensated by a change of the longitudinal velocity spread. As we will see below, this happens indeed in the considered parameter range.
- Reduction of the beta-function would be the most favorable change because it would reduce the diffraction parameter, and increase the velocity spread at the same time. Unfortunately, there are technical arguments not supporting such a change in the FLASH undulator [30].

A contour plot for the value of the diffraction parameter  $B$  for the value of beta function of 10 m and the value of beam current 1.5 kA is presented in Fig. 5. We see that the value of the diffraction parameter is  $B \gtrsim 10$  in the whole parameter space of FLASH. Figure 6 shows the ratio of the field gain  $\text{Re}(\Lambda_{10}(\omega))$  to the value of the field gain  $\text{Re}(\Lambda_{00}(\omega))$  of the fundamental mode. We see that this ratio is above 0.8 in the whole range of parameters, and we can expect significant contribution of the first azimuthal mode to the total radiation power. We can also notice relatively weak dependencies on the emittance and on the wavelength.

### Spatial Coherence

In our studies of coherent properties of FELs [3] we have found that for an optimized SASE FEL the degree of transverse coherence can be as high as 0.96. One can see from Fig. 7 that in the considered cases the degree of transverse coherence is visibly lower. We should distinguish two effects limiting the degree of transverse coherence at FLASH. The first one is called mode degeneration and was intensively discussed in this paper. This physical phenomena takes place at large values of the diffraction parameter [12]. Right plot in Fig. 8 shows the contribution of higher azimuthal modes to the total power for a specific example of emittance of 1 mm-mrad and a peak current of 1.5 kA (the results have been obtained with time-dependent, three-dimensional FEL simulation code FAST [31]). The averaged contribution of the first azimuthal modes falls down in the high gain linear regime, but to the value of 12% only, and then starts to grow in the nonlinear regime, and reaches the value of 16% at the undulator end.

The second effect is connected with a finite longitudinal coherence, it was discovered in [7] and discussed in [3, 4]. The essence of the effect is a superposition of mutually incoherent fields produced by different longitudinally uncor-

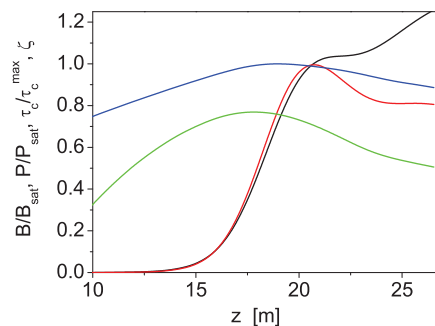


Figure 7: FLASH: evolution of the radiation power (black curve), coherence time (blue curve), degree of transverse coherence (green curve), and brilliance (red curve) along the undulator. Brilliance and radiation power are normalized to saturation values. Coherence time is normalized to maximum value of 5.5 fs. Radiation wavelength is 8 nm. Beta function is 10 m. Beam current is 1.5 kA. rms normalized emittance is 1 mm-mrad.

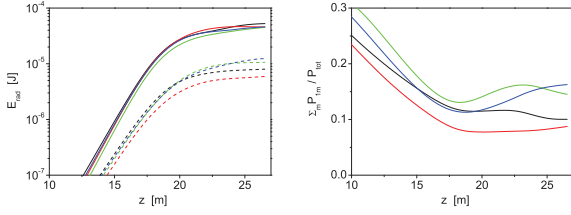


Figure 8: Left plot: evolution of the energy in the radiation pulse versus undulator length. Color codes (black to blue) correspond to different shots. Line style correspond to the total energy in the azimuthally symmetric  $\sum TEM_{0m}$  modes (solid lines), and in of the first azimuthal  $\sum TEM_{1m}$  (dashed lines). Right plot: partial contribution of the first azimuthal modes to the total radiation power,  $\sum P_{1m}/P_{tot}$ . FLASH operates at the radiation wavelength of 8 nm. Beta function is 10 m. Beam current is 1.5 kA. rms normalized emittance is 1 mm-mrad.

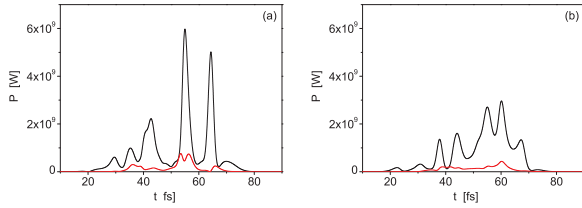


Figure 9: Temporal structure of two radiation pulses. Black lines show the power of the azimuthally symmetric modes, and the curve in the red color show the power of the first azimuthal modes. Radiation wavelength is 8 nm. Beta function is 10 m. Beam current is 1.5 kA. rms normalized emittance is 1 mm-mrad. Undulator length is 27 m.

related parts of the electron bunch. In the exponential gain regime this effect is relatively weak, but it prevents a SASE FEL from reaching full transverse coherence, even in the case when only one transverse eigenmode survives [7]. In the deep nonlinear regime beyond FEL saturation, this effect can be strong and can lead to a significant degradation of the degree of transverse coherence [3, 4]. In particular, as one can see from Fig. 7, this effect limits the degree of transverse coherence to the value about 50% when FLASH operates in the deep nonlinear regime.

### Pointing Stability and Mode Degeneration

Mode degeneration has significant impact on the pointing stability of SASE FEL. Let us illustrate this effect with a specific example for FLASH operating with an average energy in the radiation pulse of  $60 \mu\text{J}$ . The left plot in Fig. 8 shows the evolution along the undulator of the radiation energy in azimuthally symmetric modes and of the energy in the modes with azimuthal index  $n = \pm 1$ . The right plot in this figure shows the relative contribution to the total radiation energy of the modes with azimuthal index  $n = \pm 1$ . Four consecutive shots are shown here. Temporal profiles of the radiation pulses are presented in Fig. 9. Intensity distributions in the far zone for these two shots are shown

in two rows in Fig. 10. The four profiles on the left-hand side of each row show intensity distributions in the single slices for the time 40 fs, 50 fs, 60 fs, and 70 fs. The right column presents intensity profiles averaged over full shots. We see that the transverse intensity patterns in slices have a rather complicated shape due to the interference of the fields of statistically independent modes with different azimuthal indices. The shape of the intensity distributions changes on a scale of the coherence length. Averaging of slice distributions over a radiation pulse results in a more smooth distribution. However, it is clearly seen that the spot shape of a short radiation pulse changes from pulse to pulse. The center of gravity of the radiation pulse visibly jumps from shot to shot. The position of the pulse also jumps from shot to shot which is frequently referred to as poor pointing stability. Note that the effect illustrated here is a fundamental one, which takes place due to the mode degeneration when the contribution of the higher azimuthal modes to the total power is pronounced (10% to 15% in our case). Only in the case of a long radiation pulse, or after averaging over many pulses, the intensity distribution approaches asymptotically to an azimuthally symmetric shape.

### OPTIMIZED SASE FEL

Target value of interest for XFEL optimization is the field gain length of the fundamental mode. For this practically important case the solution of the eigenvalue equation for the field gain length of the fundamental mode and optimum beta function are rather accurately approximated by [3, 4, 32, 33]:

$$\begin{aligned} L_g &= 1.67 \left( \frac{I_A}{I} \right)^{1/2} \frac{(\epsilon_n \lambda_w)^{5/6}}{\lambda^{2/3}} \frac{(1 + K^2)^{1/3}}{K A_{JJ}} (1 + \delta), \\ \beta_{opt} &\approx 11.2 \left( \frac{I_A}{I} \right)^{1/2} \frac{\epsilon_n^{3/2} \lambda_w^{1/2}}{\lambda K A_{JJ}} (1 + 8\delta)^{-1/3}, \\ \delta &= 131 \frac{I_A}{I} \frac{\epsilon_n^{5/4}}{\lambda^{1/8} \lambda_w^{9/8}} \frac{\sigma_\gamma^2}{(K A_{JJ})^2 (1 + K^2)^{1/8}}, \quad (4) \end{aligned}$$

where  $\sigma_\gamma = \sigma_E/mc^2$ . In the case of negligibly small energy spread, the diffraction parameter  $B$  and parameter of betatron oscillations,  $\hat{k}_\beta$  are functions of the only parameter  $\hat{\epsilon}$  for optimized x-ray FEL. As a result, saturation characteristics of the SASE FEL written down in the dimensionless form are functions of two parameters,  $\hat{\epsilon} = 2\pi\epsilon/\lambda$  and parameter  $N_c = IL_g\lambda/(e\lambda_w c)$  defining the initial conditions for the start-up from the shot noise [3–5]. Dependence of characteristics on the value of  $N_c$  is very slow, in fact logarithmic. The values of the diffraction parameter and of the betatron motion parameter are given by (see Fig. 11):

$$B \approx 13 \times \hat{\epsilon}^{5/2}, \quad \hat{k}_\beta \approx 0.154/\hat{\epsilon}^{3/2}.$$

The maximum value of the degree of transverse (which occurs in the end of the linear regime) degrades gradually with the growth of the emittance parameter (see Fig. 12). The origin of this is the mode degeneration effect. The value of the diffraction parameter grows with the value of the emittance parameter, and starting from  $\hat{\epsilon} > 1$  the gain of the  $TEM_{10}$

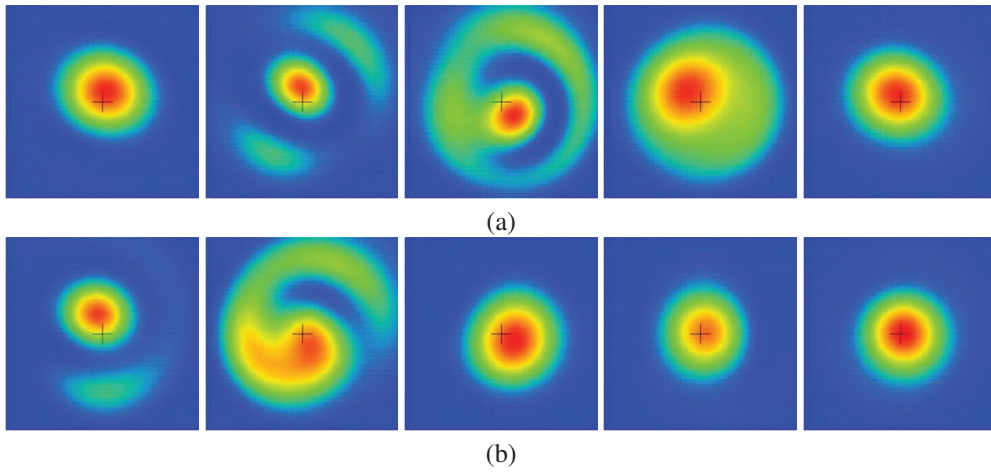


Figure 10: Profiles of the radiation intensity in the far zone. Rows correspond to specific shots with temporal structure presented in Fig. 9. Profiles on the right-hand side show average intensity over full pulse. Profiles 1 to 4 from the left-hand side show intensity distribution of selected slices corresponding to the time 40 fs, 50 fs, 60 fs, and 70 fs, respectively. Cross denotes geometrical center of the radiation intensity averaged over many shots. FLASH operates at the radiation wavelength of 8 nm. Beta function is 10 m. Beam current is 1.5 kA. rms normalized emittance is 1 mm-mrad. Undulator length is 27 m.

Table 1: Parameter Space of X-ray FELs

	LCLS	SACLA	EXFEL	SWISS FEL	PAL XFEL
Energy [GeV]	13.6	8.0	17.5	5.8	10
Wavelength [Å]	1.5	0.6	0.5	0.7	0.6
$\epsilon_n$ [mm-rad]	0.4	0.4	0.4	0.4	0.4
$\hat{\epsilon}$	1	2.7	1.5	3.4	2.1

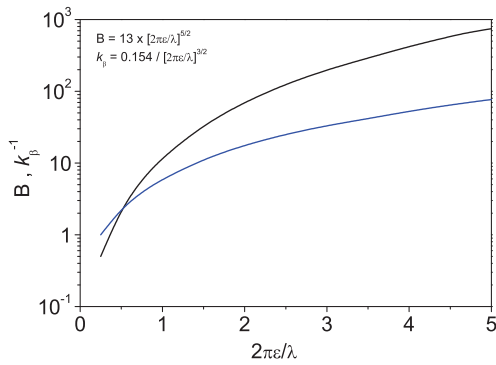


Figure 11: Optimized SASE FEL: diffraction parameter and betatron oscillation parameter versus the emittance parameter  $\hat{\epsilon} = 2\pi\epsilon/\lambda$ .

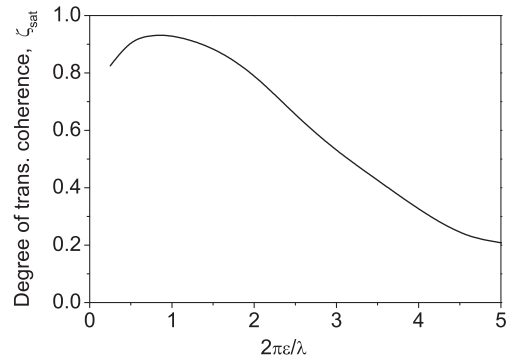


Figure 12: Optimized SASE FEL: maximum degree of transverse coherence versus the emittance parameter  $\hat{\epsilon} = 2\pi\epsilon/\lambda$ .

mode approaches closer to the gain of the ground TEM<sub>00</sub> mode (see Fig. 13). Contribution of the TEM<sub>10</sub> mode to the total power progresses with the growth of the emittance parameter (see Fig. 14). Starting from  $\hat{\epsilon} > 2$  the azimuthal modes TEM<sub>2n</sub> appear in the mode contents, and so on.

Table 1 presents comparative table of the main parameters of the x-ray FELs compiled for the shortest design wavelength [21–25]. To make comparison more simple, we assume the normalized emittance to be the same for all cases,  $\epsilon_n = 0.4$  mm-mrad. General tendency is that parameter range of hard x-ray FELs driven with low energy electron beam

corresponds to large values of the emittance parameter. As a result, output radiation will have poor spatial coherence and poor pointing stability of the photon beam. In the previous section we illustrated this problem for Free Electron Laser FLASH. Mode content of FLASH corresponds to that expected for optimized x-ray FEL operating with the value of the emittance parameter  $\hat{\epsilon}$  around 2. Situation will become much worse for larger values of  $\hat{\epsilon}$ . Note that spatial jitter is of a fundamental nature (shot noise in the electron beam), and takes place even for an 'ideal' machine.

The reasonable question arises about possible ways to suppress the mode degeneration effect. The spread of longi-

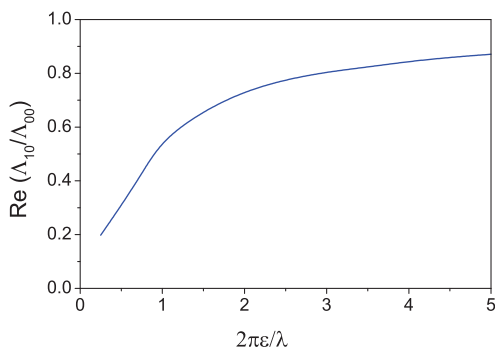


Figure 13: Optimized SASE FEL: Ratio of the gain  $\text{Re}(\Lambda_{10})/\text{Re}(\Lambda_{00})$  versus the emittance parameter  $\hat{\epsilon} = 2\pi\epsilon/\lambda$ .

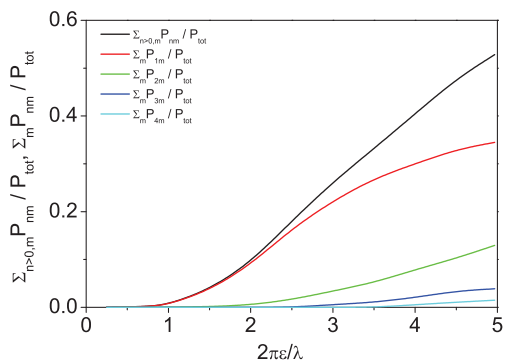


Figure 14: Optimized SASE FEL: partial contributions of the modes with azimuthal index  $m = 0 \dots 4$  to the total power versus the emittance parameter  $\hat{\epsilon} = 2\pi\epsilon/\lambda$ . SASE FEL operates in the saturation.

tudinal velocities (due to energy spread and emittance) helps to suppress high order modes thus improving transverse coherence properties. The energy spread can be increased with the laser heater [34]. Features of this effect are demonstrated with Fig. 4. However, the price for this improvement is a significant reduction of the gain of the fundamental mode and of the FEL power. A tight focusing of the electron beam in the undulator can be important for reaching higher coherence due to a reduction of the diffraction parameter and an increase of the velocity spread. This trick works for the case of FLASH, currently operating with large beta function with respect to optimum (maximum) FEL gain. Reduction of the beat function will reduce saturation length and improve spatial coherence. However, it is not the case of x-ray FEL optimized for maximum of the FEL gain. Reduction of the focusing beta function will result in the increase of the saturation length. In the end, with fixed energy of the electron beam, an available undulator length will define the level of spatial coherence and spatial jitter of the photon beam.

### ACKNOWLEDGEMENT

We thank Reinhard Brinkmann for many useful discussions.

### REFERENCES

- [1] Y.S. Derbenev, A.M. Kondratenko, E.L. Saldin, Nucl. Instrum. Methods 193, 415 (1982).
- [2] J.B. Murphy, C. Pellegrini, Nucl. Instrum. Methods A 237, 159 (1985.)
- [3] E.L. Saldin, E.A. Schneidmiller, and M.V. Yurkov, Opt. Commun. 281(2008)1179.
- [4] E.L. Saldin, E.A. Schneidmiller, and M.V. Yurkov, New J. Phys. 12 (2010) 035010, doi: 10.1088/1367-2630/12/3/035010.
- [5] E.L. Saldin, E.A. Schneidmiller, and M.V. Yurkov, Opt. Commun. 281(2008)4727.
- [6] E.A. Schneidmiller, and M.V. Yurkov, Proc. FEL 2012 Conference, <http://accelconf.web.cern.ch/AccelConf/FEL2012/papers/mopd08.pdf>.
- [7] E.L. Saldin, E.A. Schneidmiller, and M.V. Yurkov, Opt. Commun. **186**(2000)185.
- [8] G. Moore, Opt. Commun. 52, 46 (1984).
- [9] E.L. Saldin, E.A. Schneidmiller and M.V. Yurkov, Optics Commun 97(1993)272.
- [10] M. Xie, Nucl. Instrum. and Methods A 445, 59 (2000).
- [11] E.L. Saldin, E.A. Schneidmiller and M.V. Yurkov, Nucl. Instrum. and Methods A 475, 86 (2001).
- [12] E.L. Saldin, E.A. Schneidmiller, M.V. Yurkov, "The Physics of Free Electron Lasers" (Springer-Verlag, Berlin, 1999).
- [13] K.J. Kim, Phys. Rev. Lett. 57(1986)1871.
- [14] J.M. Wang and L.H. Yu, Nucl. Instrum. and Methods A250(1986)484.
- [15] S. Krinsky and L.H. Yu, Phys. Rev. A 35(1987)3406.
- [16] R. Bonifacio et al., Nucl. Instrum. and Methods **A341**(1994)181.
- [17] R. Bonifacio et al., Phys. Rev. Lett. **73**(1994)70.
- [18] E.L. Saldin, E.A. Schneidmiller and M.V. Yurkov, Opt. Commun. 148(1998)383.
- [19] K.J. Kim, Phys. Rev. Lett. **57**(1986)1871.
- [20] E.L. Saldin, E.A. Schneidmiller and M.V. Yurkov, Phys. Rev. ST-AB 9(2006)030702
- [21] P. Emma et al. Nature Photonics 4, 641 (2010).
- [22] T. Ishikawa et al., Nature Photonics 6, 540 (2012).
- [23] R. Ganter (Ed.), Swiss FEL Conceptual Design Report, PSI Bericht Nr. 10-04, April 2012.
- [24] H.S. Kang, K.W. Kim, I.S. Ko, Proc. IPAC 2014 Conf., paper THPRO019 (2014), <http://accelconf.web.cern.ch/AccelConf/IPAC2014/papers/thpro019.pdf>
- [25] M. Altarelli et al. (Eds.), XFEL: The European X-Ray Free-Electron Laser. Technical Design Report, Preprint DESY 2006-097, DESY, Hamburg, 2006 (see also <http://xfel.desy.de>).
- [26] W. Ackermann et al., Nature Photonics **1**(2007)336

- [27] K. Honkavaara, B. Faatz, J. Feldhaus, S. Schreiber, R. Treusch, M. Vogt, Proc. FEL2014 Conference, Basel, Switzerland, 2014, web05. <http://accelconf.web.cern.ch/AccelConf/FEL2014/papers/web05.pdf>
- [28] E.A. Schneidmiller and M.V. Yurkov, J. Mod. Optics (2015). DOI: 10.1080/09500340.2015.1066456.
- [29] R. Bonifacio, C. Pellegrini and L.M. Narducci, Opt. Commun. 50 (1984) 373.
- [30] B. Faatz and E. Prat, Alternative Focusing for FLASH, TESLA FEL Report 2009-10, DESY, Hamburg, 2009.
- [31] E.L. Saldin, E.A. Schneidmiller, and M.V. Yurkov, Nucl. Instrum. and Methods A **429**(1999)233.
- [32] E.L. Saldin, E. A. Schneidmiller, and M.V. Yurkov, Opt. Commun. 235(2004)415.
- [33] E. A. Schneidmiller, and M.V. Yurkov, Phys. Rev. ST AB, 15, 080702 (2012).
- [34] E.L. Saldin, E.A. Schneidmiller, and M.V. Yurkov, Nucl. Instrum. and Methods A 528, 355 (2004).